Available online at www.sciencedirect.com
SCIENCE DIRECT®
Synthetic Metals 151 (2005) 65–72
SYNTHETIC METALS
www.elsevier.com/locate/synmet

On metallic characteristics in some conducting polymers☆

P.K. Kahol[a,b,*], J.C. Ho[a], Y.Y. Chen[c], C.R. Wang[c], S. Neeleshwar[c], C.B. Tsai[c], B. Wessling[d]

[a] *Department of Physics, Wichita State University, Wichita, KS 67260-0032, USA*
[b] *Department of Chemistry, Wichita State University, Wichita, KS, USA*
[c] *Institute of Physics, Academia Sinica, Taipei, Taiwan*
[d] *Ormecon GmbH, Ferdinand-Harten-Str. 7, D-22949 Ammersbeck, Germany*

Received 8 November 2004; received in revised form 21 January 2005; accepted 7 March 2005
Available online 11 May 2005

Abstract

Polyaniline (PANI) exhibits a dc conductivity $\sigma \approx 10^{-1}$ S/cm when it is doped with poly(styrenesulfonic acid) (PSSA) such that the number of sulfonate groups per two-ring PANI unit (y) is 2. On increasing the dopant amount to $y = 12$, σ drops to 10^{-5} S/cm. The EPR-derived magnetic susceptibility of these two conducting polymers gives nearly the same density of states at the Fermi level $N(E_F) \approx 0.65 \pm 0.05$ states/eV 2-rings. The corresponding electronic specific heat coefficient as calculated from this $N(E_F)$ value does not appear to be inconsistent with the results from low temperature calorimetric measurements. Similarly, with y' defined as the number of sulfonate groups per three-ring PEDOT unit, PSSA-doping of poly(ethylenedioxythiophene) (PEDOT) yields different $\sigma \approx 10^{-1}$ and 10^{-5} S/cm at $y' = 5.7$ and 45.9, respectively, but the same $N(E_F) \approx 0.55 \pm 0.05$ states/eV 3-rings. These observations suggest that the additional dopants, which help with dispersion in processing conducting polymers, do not alter the metallic domains but are located in the disordered regions surrounding them. The $N(E_F)$ values also remain practically the same between *p*-toluenesulfonic acid (PTSA) doped PANI and its dispersed blend in poly(methylmethacrylate) (PMMA), as well as for PEDOT–PTSA before and after its being subjected to an additional dispersion step.

PACS: PACS numbers: 72.80.Le; 76.30; 65.60.+a

Keywords: Magnetic susceptibility; Heat capacity; Density of states; Electron paramagnetic resonance; Conductivity; Organic polymers

1. Introduction

Conducting polymers and high-T_c superconductors are among the most rewarding materials discovered in recent years. Both have led to Nobel prizes. While an exceedingly large amount of experimental and theoretical work has helped elucidate the superconductivity mechanism and related phenomena, high temperature superconductors still face technical barriers toward application. In contrast, a number of technologies based on conducting polymers are now in service. Current research programs are mostly concerned with syntheses, morphology and better characterization [1,2]. However, realizing the unavoidable complications associated with polymeric materials, experimental investigations of fundamental properties have been somewhat limited.

Unlike saturated polymers that have all four valence electrons of carbon tied up in covalent bonds, the classical example of *trans*-polyacetylene in the family of conducting polymers identifies its unpaired π-electrons as a source for intrinsic conductivity. Because of electron–lattice interactions, structural distortions occur, inducing polarons, bipolarons and solitons [3,4]. Suitable oxidation (p-doping) and reduction (n-doping) of certain polymers have been demonstrated to result in a wide range of electrical conductivity σ

☆ Some of the results presented in this paper were presented at the International Conference on the Science and Technology of Synthetic Metals held at the University of Wollongong, Australia, 28 June to 2 July 2004.

* Corresponding author. Tel.: +1 316 978 6244; fax: +1 316 978 3253.
E-mail address: Pawan.kahol@wichita.edu (P.K. Kahol).

0379-6779/$ – see front matter © 2005 Elsevier B.V. All rights reserved.
doi:10.1016/j.synthmet.2005.03.017

from 10^{-13} to 10^{5} S/cm. In comparison, copper has a room-temperature σ of 6×10^{5} S/cm.

The conductivity of emeraldine-base polyaniline has been found to increase from 10^{-10} to 10^{2} S/cm on doping [5]. It has been suggested that at sufficiently high doping levels, conducting polymers are comprised of nano-sized "metallic" domains separated by disordered regions [6]. A metallic domain is a region in which the polymer chains are highly coupled and show interchain coherence length of the order of 5 nm. Although conducting polymers are susceptible to high degrees of disorder and inhomogeneities, which complicate transport property studies, the characteristics of their metallic domains continues to attract interest and attention [1–4].

One basic parameter for metallic characterization is the density of states at the Fermi level, $N(E_F)$, which has been evaluated for various conducting polymers through electron paramagnetic resonance (EPR) spectroscopy [4,7–10], static magnetic measurements [6,11–13] or low temperature calorimetry [14,15]. Using such techniques, this study aims at determining the effect on $N(E_F)$ due to excessive poly(styrenesulfonic acid) (PSSA) doping, which helps in dispersion processing, in polyaniline (PANI) and poly(ethylenedioxythiophene) (PEDOT). Electrical conductivity of the PSSA doped PEDOT can be varied also over a wide range using different molar ratios of PEDOT and PSSA.

Comparisons are also made on *p*-toluenesulfonic acid (PTSA)-doped PANI before and after their being subjected to a special dispersion process, and before and after their being blended and dispersed in poly(methylmethacrylate) (PMMA).

2. Experimental

Fig. 1 shows the chemical structures of the various materials used in the study.

Two dispersible PSSA-doped PANI samples were obtained from Ormecon [16]. With the formula units of PANI and PSSA defined as $–(C_6H_4N–C_6H_5N)–$ and $–CH_2CH(C_6H_4SO_3)–$, the two samples have different number of sulfonate groups per two-ring PANI unit, $y = 2$ and 12. They will be identified as PANI–PSSA-2 and PANI–PSSA-12, respectively. The larger y value reflects a much more excessive doping level.

Two dispersion-processed PEDOT–PSSA samples from Starck [17], under their trade names AI 4071 and CH 8000, were dried into powders. Both are excessively doped, but at appreciably different levels. With the formula unit of PEDOT defined as $–[(C_6H_4O_2S)_3]–$, the number of sulfonate groups per three-ring PEDOT unit y' is 5.7 for AI 4071 and 45.9 for CH 8000. We will henceforth refer AI 4071 as PEDOT–PSSA-6 and CH 8000 as PEDOT–PSSA-46.

Two PTSA-doped PANI samples, one in a non-dispersed condition (PANI–PTSA-1) and another one having been blended and dispersed in PMMA (PANI–PTSA–PMMA), were obtained from Ormecon [16]. There is one sulfonate group per two-ring PANI unit. Dispersion in PMMA enhances conductivity and induces even a metal–insulator transition at lower temperatures [18].

The last sample is a non-dispersed PEDOT doped with PTSA (PEDOT–PTSA-1.5) having 1.5 sulfonate groups per three-ring PEDOT unit. Comparison is made after its being subjected to an extra dispersion step, thus identified as PEDOT–PTSA-1.5Q.

A computer controlled X-band Bruker EMX 6/1 spectrometer (9.5 GHz) was used for EPR measurements. An Oxford ESR900 cryostat under ITC503 control was used for controlling temperature down to 4.2 K. The derivative intensity data following an EPR experiment were integrated twice. This result was divided by the double integral of the derivative EPR signal for a K_3CrO_8 standard [19] to obtain a value for the magnetic susceptibility. The absolute uncertainty in the EPR obtained $N(E_F)$ values is primarily due to mass measurements of the K_3CrO_8 crystal and its solution in a capillary. This error is small and estimated to be approximately 10%.

SQUID was employed also to obtain magnetic susceptibility. Specific heat measurements were made using a thermal-relaxation type microcalorimeter in a He^3 cryostat, the details of which were given in an earlier paper [15].

3. Results and discussion

3.1. Electrical conductivity

The dc electrical conductivity measurements were made on compressed pellets of the samples using the standard four-probe technique. Fig. 2(a)–(d) show the temperature dependence of the dc conductivity for the four samples PEDOT–PSSA-6, PEDOT–PSSA-46, PANI–PSSA-2, and PANI–PSSA-12, respectively. The room-temperature electrical conductivity is 10^{-1} S/cm for PEDOT–PSSA-6 and 2×10^{-5} S/cm for PEDOT–PSSA-46. For PANI–PSSA-2 and PANI–PSSA-12, it is 0.5 and 7×10^{-6} S/cm, respectively. Clearly, excess doping leads to a significant decrease in conductivity. With the materials in the vicinity of metal–insulator (MI) transition, Fig. 3 shows the temperature dependence of reduced activation energy W defined as $\Delta \ln \sigma / \Delta \ln T$. In such a plot, a positive slope at low temperatures is considered as an indication of metallic characteristics. Accordingly, PEDOT–PSSA-6 and PANI–PSSA-2 are on the metallic side, PANI–PSSA-12 is near the boundary, and PEDOT–PSSA-46 is on the insulating side of the MI transition. PANI–PTSA–PMMA has also been shown earlier to be on the metallic side [18].

PEDOT–PTSA-1.5 has a dc conductivity of 90 S/cm, following an extra dispersion step, the conductivity increases to 240 S/cm in PEDOT-PTSA-1.5Q.

Most of the samples mentioned above including PANI–PSSA-2, PEDOT–PSSA-6, PANI–PTSA–PMMA and PEDOT–PTSA-1.5Q, which have reasonably good conduc-

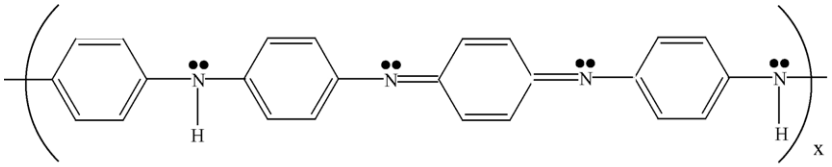

(a) Polyaniline (PANI) in the emeraldine-base form

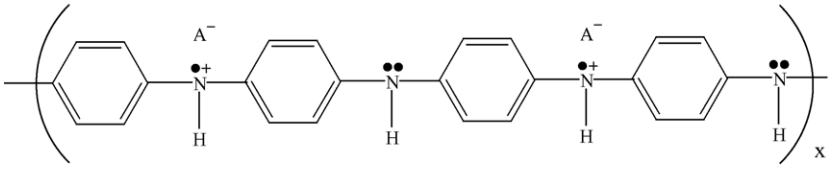

(b) Conducting PANI in the emeraldine-salt form. A^- is the dopant anion.

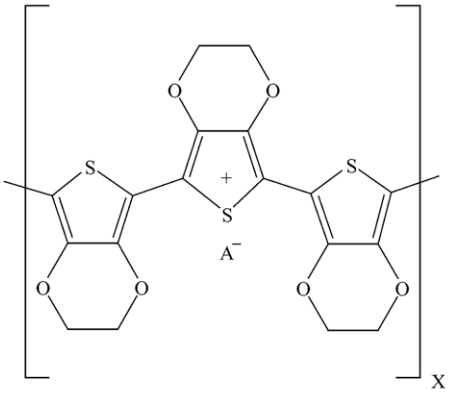

(c) Doped poly(ethylenedioxythiophene) (PEDOT). A^- is the dopant anion.

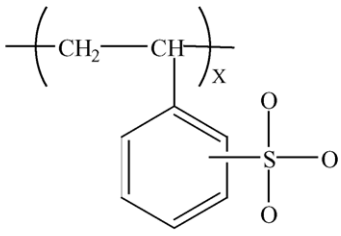

(d) Poly(styrenesulfonate) ion (PSSA)

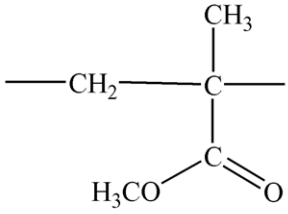

(e) Poly(methylmethacrylate) (PMMA)

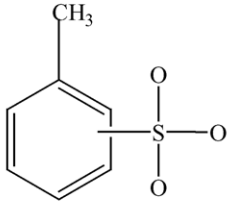

(f) p-toluenesulfonate ion (PTSA)

Fig. 1. Chemical structure of materials used in the present study.

tivity or behave as being on the metallic side of the MI transition, are not conventional metals in terms of mean free path. They are instead comprised of metallic domains or "islands", which are surrounded by disordered regions. The disordered regions are quasi one-dimensional, and charge carriers hop between chains and along chains. Charge carriers are confined in the metallic regions as long as the on-chain localization length is smaller than the distance between the metallic regions or islands. As the on-chain localization length increases due to favorable chain morphology in the disordered regions, the charge carriers can diffuse among the metallic regions.

Questions arise as to what extent the excess doping, which greatly reduces the conductivity, would affect the metallic domains. The answer is difficult to obtain only from transport property measurements. Rather, magnetic and calorimetric studies seem to be in order to shed some light in this respect.

3.2. Electron paramagnetic resonance

One major contribution to the magnetic susceptibility χ of most metallic systems is the temperature-independent Pauli susceptibility, χ_P. Being a characteristic signature of

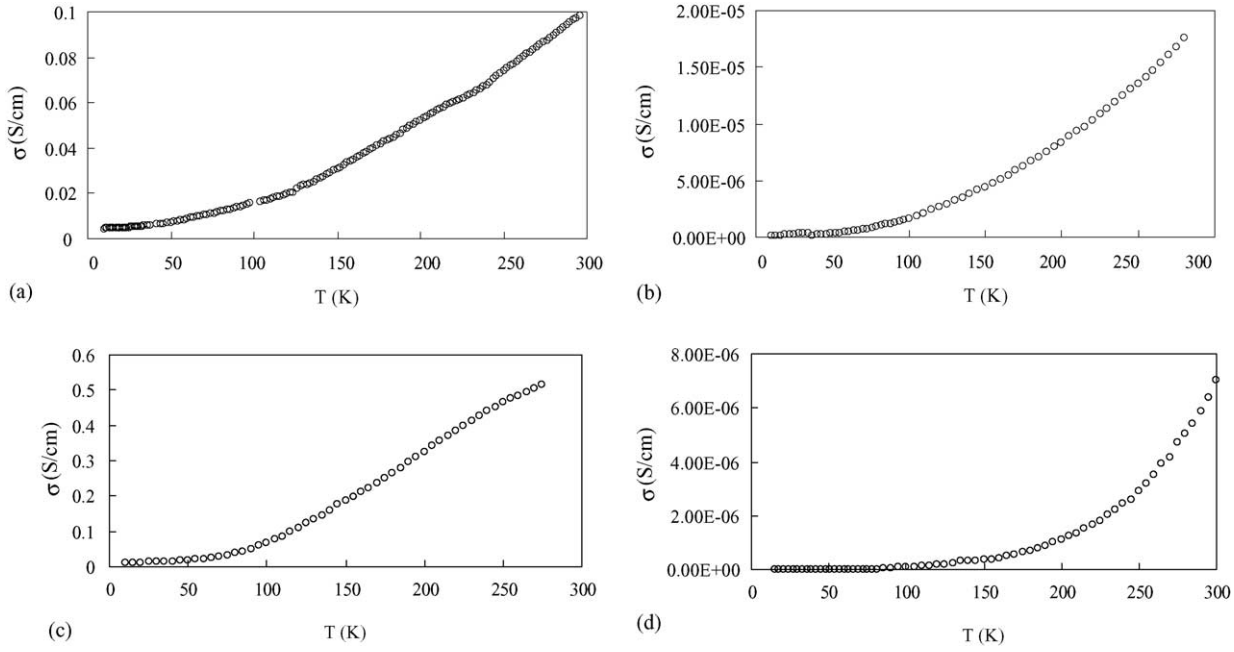

Fig. 2. Temperature dependence of dc conductivity σ as a function of temperature for (a) PEDOT–PSSA-6, (b) PEDOT–PSSA-46, (c) PANI–PSSA-2, and (d) PANI–PSSA-12.

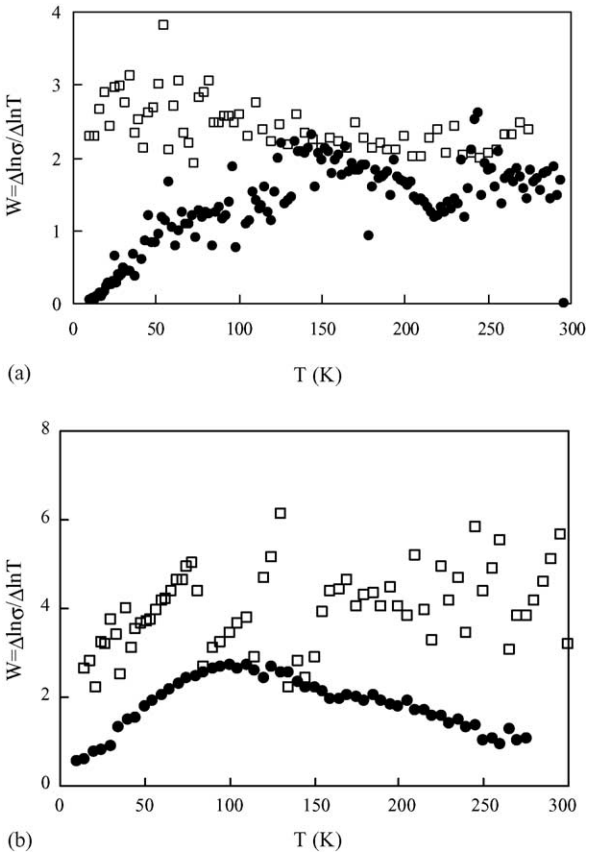

Fig. 3. Temperature dependence of reduced activation energy W for (a) PEDOT–PSSA-6 (circles) and PEDOT–PSSA-46 (squares), and (b) PANI–PSSA-2 (circles) and PANI–PSSA-12 (squares).

the presence of delocalized spins, χ_P is directly proportional to $N(E_F)$ for both spin directions through the relation $\chi_P = \mu_B^2 N(E_F)$ with μ_B being the Bohr magneton [4]. In contrast to the static measurements, e.g. SQUID to be described below, the technique of EPR measures only the spin part of magnetic susceptibility. For disordered conducting polymeric systems, the measured susceptibility is expected to be a sum of Curie and Pauli components: $\chi = N\mu_B^2/k_B T + \chi_P$ or $\chi T = (N\mu_B^2/k_B) + [\mu_B^2 N(E_F)]T$, with N being the number of Curie-type spins and k_B the Boltzmann constant. Accordingly, from a χT versus T plot, χ_P and hence $N(E_F)$ can be obtained from the slope of a straight line fit, while its intercept would yield the value of N. $N(E_F)$ is expressed here in states/eV formula unit, where the formula unit will correspond to a three-ring unit for PEDOT and a two-ring unit for PANI. The relatively small values of N are not a main concern of this study.

To first examine the effect of excess doping on metallic characteristics, Fig. 4 shows the EPR-derived magnetic susceptibility values for PSSA-doped PEDOT and PANI. The temperature dependence of χT can be indeed represented by a straight line in each case. Results from a linear regression of the χT data can be summarized as follows: $N(E_F) \approx 0.55 \pm 0.05$ states/eV 3-rings for PEDOT–PSSA-6 and 0.50 ± 0.05 states/eV 3-rings for PEDOT–PSSA-46, with corresponding $N \approx 0.004$ and 0.002 per formula unit, respectively. PANI–PSSA-2 and PANI–PSSA-12 have practically the same $N(E_F) \approx 0.65 \pm 0.10$ states/eV 2-rings and $N \approx 0.003$ and 0.005 per formula unit, respectively. It appears that the excess doping does not affect the density of states at the Fermi level in either the PANI or the PEDOT systems.

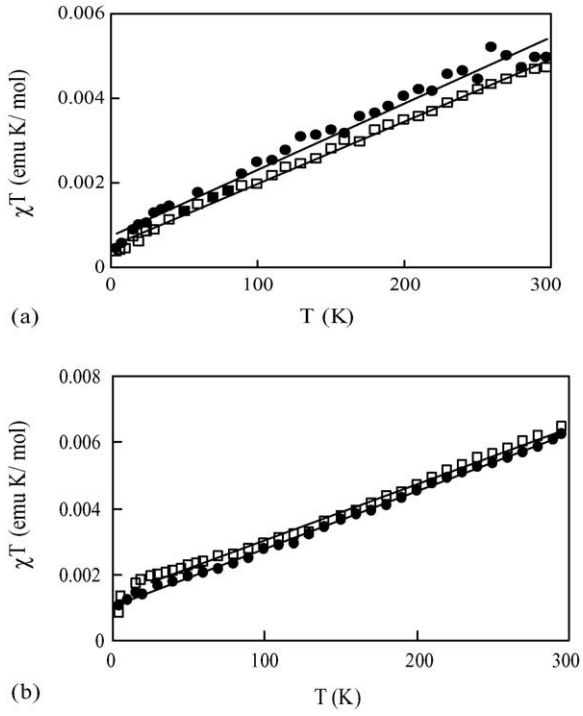

Fig. 4. EPR-derived magnetic susceptibility as a function of temperature for (a) PEDOT–PSSA-6 and PEDOT–PSSA-46, and (b) PANI–PSSA-2 and PANI–PSSA-12. Each straight line represents linear regression of the χT data.

A small difference in $N(E_F)$ values appears in Fig. 5. It is 2.0 ± 0.10 states/eV 2-rings for PTSA doped PANI (PANI–PTSA-1) and 2.2 ± 0.10 states/eV 2-rings for its dispersed blend in PMMA (PANI–PTSA–PMMA).

Again, the linear fit for the χT versus T plot in Fig. 6 indicates that the $N(E_F)$ value changes from 0.65 ± 0.05 states/eV 3-rings for PEDOT-PTSA-1.5 to only a slightly higher value of 0.75 ± 0.05 states/eV 3-rings for PEDOT-PTSA-1.5Q, which had been subjected to an extra dispersion step.

All $N(E_F)$ values thus obtained are listed in Table 1.

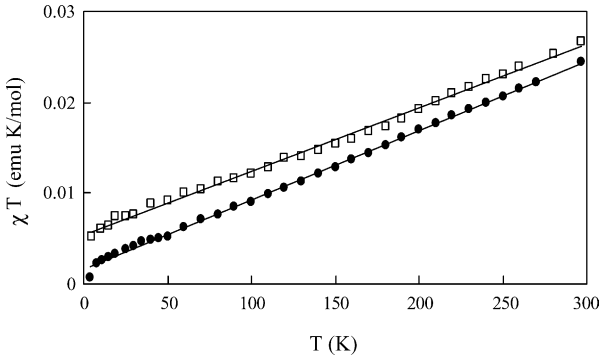

Fig. 5. EPR-derived magnetic susceptibility as a function of temperature for PANI–PTSA-1 and PANI–PTSA–PMMA. Each straight line represents linear regression of the χT data.

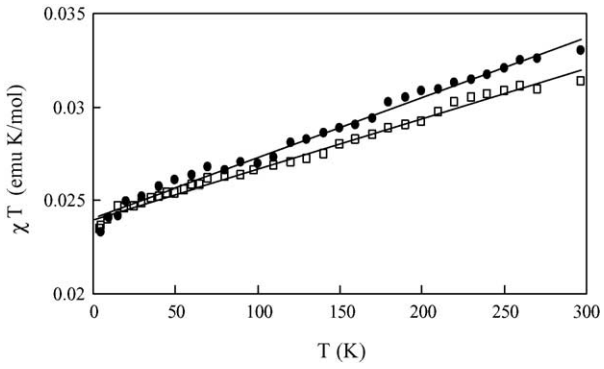

Fig. 6. EPR-derived magnetic susceptibility as a function of temperature for PEDOT–PTSA-1.5 and PEDOT–PTSA-1.5Q. Each straight line represents linear regression of the χT data.

Table 1
Comparison of $N(E_F)$ values obtained from EPR and heat capacity measurements

Sample	$N(E_F)$ from EPR (states/eV formula unit)
PEDOT–PSSA-6	0.55 ± 0.05
PEDOT–PSSA-46	0.50 ± 0.05
PANI–PSSA-2	0.65 ± 0.05
PANI–PSSA-12	0.70 ± 0.05
PANI–PTSA-1	2.0 ± 0.1
PANI–PTSA–PMMA	2.2 ± 0.1
PEDOT–PTSA-1.5	0.65 ± 0.05
PEDOT–PTSA-1.5-Q	0.75 ± 0.05

3.3. SQUID magnetometry

Like a "force" magnetometer, SQUID yields the total magnetic susceptibility that is comprised of several contributions including intrinsic core diamagnetic χ_{dia}. As shown in Fig. 7, some of the conducting polymers reported in the present study have negative or near zero total susceptibility. Obviously, the core diamagnetism is appreciable, and needs to be subtracted from the total susceptibility to allow the determination of $N(E_F)$-related Pauli contribution. To

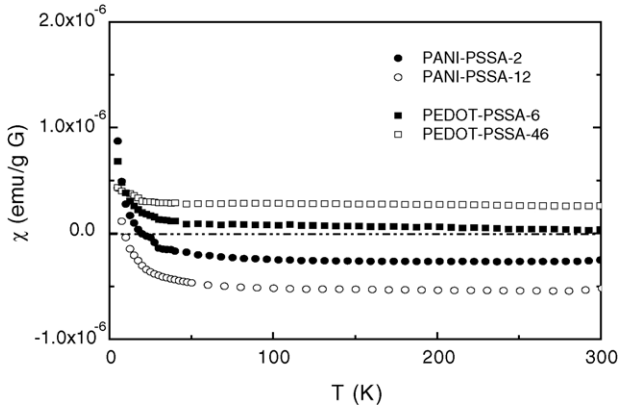

Fig. 7. Magnetic susceptibility data from SQUID measurements revealing significant contributions from core diamagnetism.

do so one often relies on a set of empirically derived parameters generally referred to as Pascal constants (e.g., -6.00×10^{-6} emu/mol for C, -4.61×10^{-6} emu/mol for O, and -15.0×10^{-6} emu/mol for S) and constitutive corrections (e.g., $+5.5 \times 10^{-6}$ emu/mol for C=C bond, $+8.15 \times 10^{-6}$ emu/mol for C=N bond, and -3.07×10^{-6} emu/mol for C shared by two rings) [20]. The values of the Pascal's constants have been deduced from examining the susceptibilities of various compounds, and uncertainties in the literature values can lead to significantly erroneous estimates of χ_{dia} and consequently $N(E_F)$ for conducting polymers because they are comprised of a large number of atoms and chemical bonds. The detailed analysis of the data in Fig. 7 is in progress and will be reported later if meaningful results can be arrived. Meanwhile, it is deemed worthy to point out such difficulties that one would encounter using the static magnetic measurements on polymeric materials.

3.4. Low temperature specific heat

At sufficiently low temperatures the specific heat of a normal metallic solid generally follows a simple relation: $C = \gamma T + \beta T^3$ or $C/T = \gamma + \beta T^2$. The electronic specific heat coefficient γ, as to be determined from the intercept of a linear fit in a C/T versus T plot, is a measure of $N(E_F)$ (in states/eV formula unit) = 0.424γ (in mJ/(mol K^2)) for both spin directions, and the slope β is the lattice specific heat coefficient.

Specific heat data in Fig. 8 for PEDOT–PSSA-6 and PEDOT–PSSA-46 reveal some kind of anomalies below approximately 2 K. The lattice contribution is apparently the dominating term, particularly with the higher dopant content. Further uncertainty in the high-temperature limit of the T^3-dependence for lattice specific heat makes it harder to obtain unambiguous values of $N(E_F)$. Therefore,

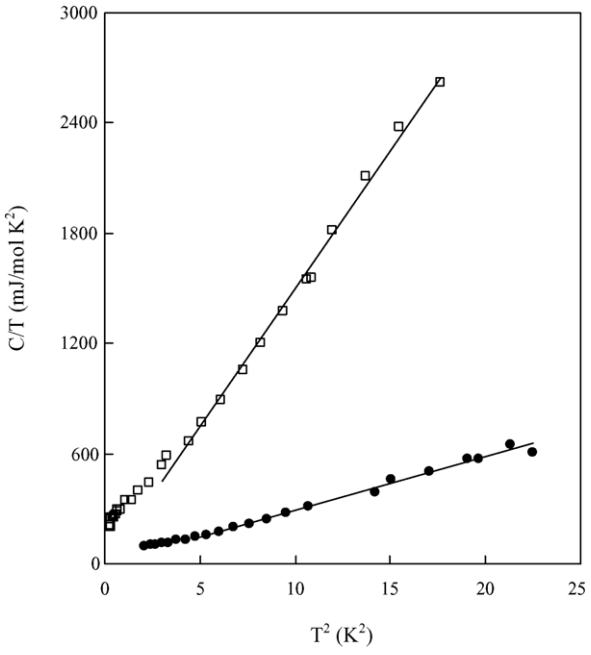

Fig. 8. Analysis of the temperature dependence of specific heat for PEDOT–PSSA-6 and PEDOT–PSSA-46. Each straight line represents linear regression results of the C/T data above the lower-temperature anomalies.

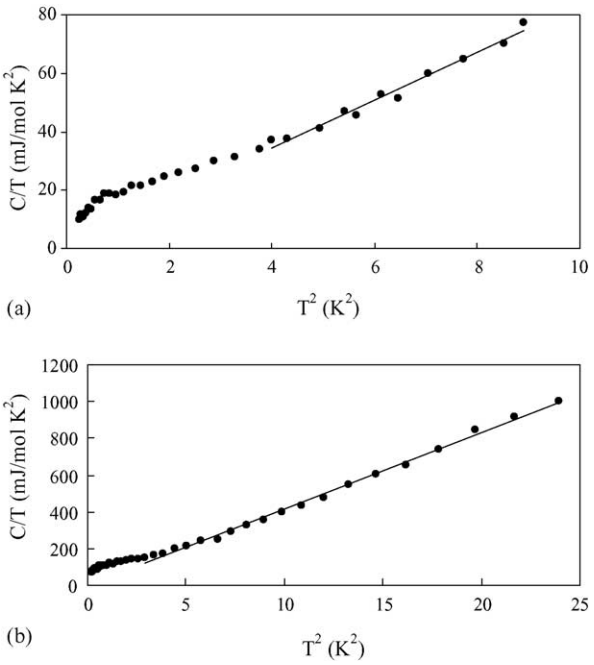

Fig. 9. Analysis of the temperature dependence of specific heat for (a) PANI–PSSA-2, and (b) PANI–PSSA-12. Each straight line represents linear regression of the C/T data above the lower-temperature anomalies.

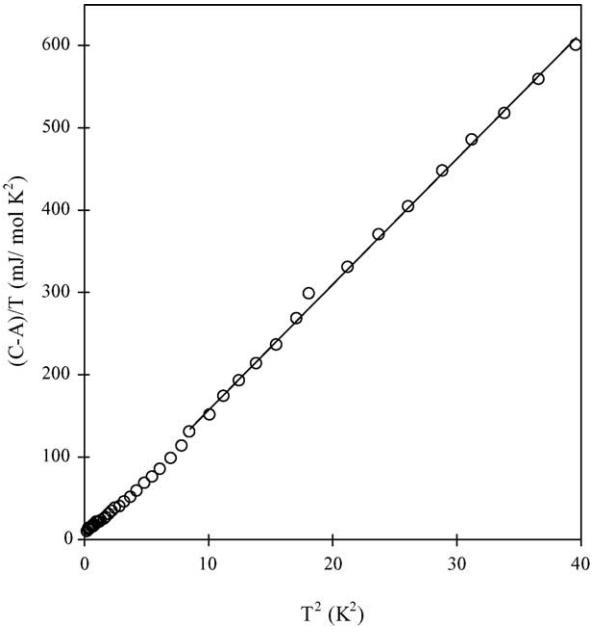

Fig. 10. Analysis of the temperature dependence of specific heat for PANI–PTSA-1. The straight line represents linear regression of the $(C - A)/T$ data above the lower-temperature anomalies. A is a constant as explained in Ref. [15].

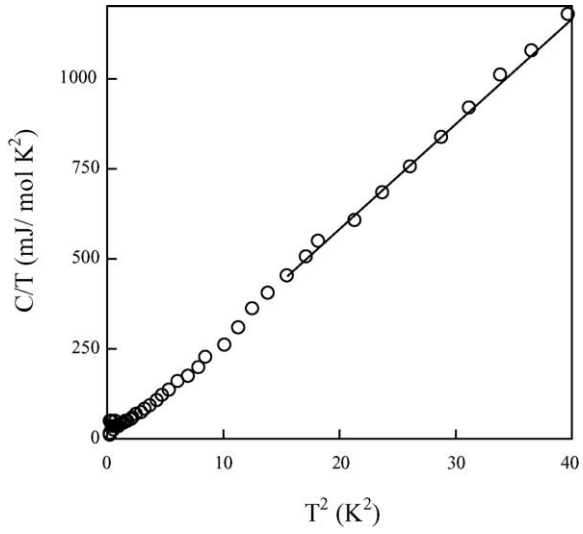

Fig. 11. Analysis of the temperature dependence of specific heat for PANI–PTSA–PMMA. The straight line represents linear regression of the C/T data above the lower-temperature anomalies.

a different approach is taken by first calculating a value of $\gamma = N(E_F)/0.424 = 1.2$ mJ/(mJ mol K^2) from the EPR results. It is then used as the predetermined intercept for a straight line fit to each set of C/T versus T^2 data above the anomalous region in Fig. 8. Indeed, the straight line fit by linear regression yields a quite acceptable coefficient of determination $R^2 = 0.9953$ for PEDOT–PSSA-6 and $R^2 = 0.9898$. Same procedures are applied to other systems with calculated $\gamma = 1.50$ mJ/(mol K^2) for PANI–PSSA-2 and PANI–PSSA-12, and 5.0 mJ/(mol K^2) for PANI–PTSA-1 and PANI–PTSA–PMMA. Again, as shown in Figs. 9–11, a good linear fit above lower-temperature anomalies prevails in each case, implying that the calculated γ and thus the $N(E_F)$ values are consistent with the specific heat data. In this respect, the low temperature calorimetry provides a complementary support to the EPR study in determining the metallic characteristics of the conducting polymers.

4. Conclusions

A much higher doping level in PANI–PSSA-12 results in four orders of magnitude lower electrical conductivity than that of PANI–PSSA-2, but the same density of states at the Fermi level. Same observation is made between PEDOT–PSSA-46 and PEDOT–PSSA-6. The additional dopant must then be located in the disordered regions surrounding the (metallic) primary particles [21,22]. Meanwhile, they help the particles disperse in aqueous media, an important concern in material processing. Although the primary particle size in PANI is around 10 nm, agglomerates of the particles (or secondary particles) having an average size of 40 nm [23] are nearly always found. PEDOT, on the other hand, has a particle size in the range 80–100 nm for PEDOT–PSSA-6 and around 20 nm for PEDOT–PSSA-46 [17].

When PANI–PTSA-1 is blended with PMMA to obtain PANI–PTSA–PMMA, the treatment promotes dispersion of metallic particles, but $N(E_F)$ remains the same. It could be an indication that the special dispersion treatment does not significantly alter the morphology of the primary particles. Both PANI–PSSA-2 and PANI–PSSA-12 have been subjected to the above mentioned additional dispersion step, and both are found to have the same $N(E_F)$ values. Same is the case between PEDOT–PTSA-1.5 and PEDOT–PTSA-1.5Q, where the latter material is obtained from the former by subjecting it to an additional dispersion step.

Acknowledgments

Acknowledgment is made to the Petroleum Research Fund, administered by the American Chemical Society (ACS-PRF#36902-B7), and the National Research Council, Taiwan (NSC90-2112-M-001-055), for partial support of this work.

References

[1] H.S. Nalwa (Ed.), Handbook of Organic Conductive Molecules and Polymers, vol. 1–4, Wiley, New York, 1997.
[2] T.A. Skotheim, R.L. Elsenbaumer, J.R. Reynolds (Eds.), Handbook of Conducting Polymers, vol. 2nd, Marcel Dekker Inc., New York, 1998.
[3] Y. Lu, Solitons and Polarons in Conducting Polymers, World Scientific Publishing Co. Inc., Singapore, 1988.
[4] P.K. Kahol, W.G. Clark, M. Mehring, in: H.G. Kiess (Ed.), Conjugated Conducting Polymers, Springer Series in Solid State Sciences, vol. 102, Springer-Verlag, Berlin, 1992, p. 1002.
[5] J.C. Chiang, A.G. MacDiarmid, Synth. Met. 13 (1986) 193.
[6] J.M. Ginder, A.F. Richter, A.G. MacDiarmid, A.J. Epstein, Solid State Commun. 63 (1987) 97.
[7] K. Mizoguchi, S. Kuroda, Handbook of Organic Conductive Molecules and Polymers, vol. 3, Wiley, New York, 1997, p. 251.
[8] Z.H. Wang, A. Ray, A.G. MacDiarmid, A.J. Epstein, Phys. Rev. B 43 (1991) 4373.
[9] K.R. Brenneman, J. Feng, Y. Zhou, A.G. MacDiarmid, P.K. Kahol, A.J. Epstein, Synth. Met. 101 (1999) 785.
[10] P.K. Kahol, K.K. Satheesh Kumar, S. Geetha, D.C. Trivedi, Synth. Met. 139 (2003) 191.
[11] P.K. Kahol, H. Guan, B.J. McCormick, Phys. Rev. B 44 (1991) 103.
[12] P.K. Kahol, A. Raghunathan, B.J. McCormick, Synth. Met. 140 (2004) 261.
[13] D. Chaudhuri, A. Kumar, D.D. Sarma, M. Garcia-Hernandez, J. Joshi, S.V. Bhat, Appl. Phys. Lett. 82 (2003) 1733.
[14] D. Moses, A. Denenstein, A. Pron, A.J. Heeger, A.G. MacDiarmid, Solid State Commun. 36 (1980) 219.
[15] A. Raghunathan, P.K. Kahol, J.C. Ho, Y.Y. Chen, Y.D. Yao, Y.S. Lin, B. Wessling, Phys. Rev. B 58 (1998) R15955.
[16] Ormecon Chemie (a subsidiary of Zipperling Kessler & Co.), Ammersbek, Germany.
[17] H.C. Starck of the Bayer Group.

[18] W. Lennartz, T. Mietzner, G. Nimtz, B. Wessling, Synth. Met. 119 (2001) 425.
[19] N.S. Dalal, J.M. Millar, M.S. Jagadeesh, M.S. Seehra, J. Chem. Phys. 74 (1981) 1916.
[20] A. Earnshaw, Introduction to Magnetochemistry, Academic Press, London, 1968, p. 6.
[21] Z.H. Wang, H.H.S. Javadi, A. Ray, A.G. MacDiarmid, A.J. Epstein, Phys. Rev. B 42 (1990) 541.
[22] P.K. Kahol, A.J. Dyakonov, B.J. McCormick, Synth. Met 89 (1997) 17.
[23] B. Wessling, Synth. Met. 135–136 (2003) 265.